

Article

# Stability Analysis and Hopf Bifurcation of a Delayed Diffusive Predator–Prey Model with a Strong Allee Effect on the Prey and the Effect of Fear on the Predator

Yining Xie <sup>1</sup>, Jing Zhao <sup>1</sup> and Ruizhi Yang <sup>2,\*</sup> 

<sup>1</sup> School of Mechanical and Electrical Engineering, Northeast Forestry University, Harbin 150040, China; yiningxie@nefu.edu.cn (Y.X.)

<sup>2</sup> Department of Mathematics, Northeast Forestry University, Harbin 150040, China

\* Correspondence: yangrz@nefu.edu.cn

**Abstract:** In this paper, we propose a diffusive predator–prey model with a strong Allee effect and nonlocal competition in the prey and a fear effect and gestation delay in the predator. We mainly study the local stability of the coexisting equilibrium and the existence and properties of Hopf bifurcation. We provide bifurcation diagrams with the fear effect parameter ( $s$ ) and the Allee effect parameter ( $a$ ), showing that the stable region of the coexisting equilibrium increases (or decreases) with an increase in the fear effect parameter ( $s$ ) (or the Allee effect parameter ( $a$ )). We also show that gestation delay ( $\tau$ ) can affect the local stability of the coexisting equilibrium. When the delay ( $\tau$ ) is greater than the critical value, the coexistence equilibrium loses its stability, and bifurcating periodic solutions appear. Whether the bifurcated periodic solution is spatially homogeneous or inhomogeneous depends on the fear effect parameter ( $s$ ) and the Allee effect parameter ( $a$ ). These results show that the fear effect parameter ( $s$ ), the Allee effect parameter ( $a$ ), and gestation delay ( $\tau$ ) can be used to control the growth of prey and predator populations.

**Keywords:** delay; Hopf bifurcation; predator–prey; Allee effect

**MSC:** 34K18; 35B32



**Citation:** Xie, Y.; Zhao, J.; Yang, R. Stability Analysis and Hopf Bifurcation of a Delayed Diffusive Predator–Prey Model with a Strong Allee Effect on the Prey and the Effect of Fear on the Predator. *Mathematics* **2023**, *11*, 1996. <https://doi.org/10.3390/math11091996>

Academic Editor: Irina Bashkirtseva

Received: 16 March 2023

Revised: 17 April 2023

Accepted: 19 April 2023

Published: 23 April 2023



**Copyright:** © 2023 by the authors. Licensee MDPI, Basel, Switzerland. This article is an open access article distributed under the terms and conditions of the Creative Commons Attribution (CC BY) license (<https://creativecommons.org/licenses/by/4.0/>).

## 1. Introduction

Scholars have long been committed to using mathematical methods to explain and predict biological phenomena [1–4]. The analysis of predator–prey models is a research subject that has recently attracted considerable attention [5–8] from mathematicians and biologists. In order to better describe the law of changes in a population, many scholars have used differential equations to build predator–prey models and have introduced different parameters in order to consider biological factors. Considering that the internal mating of a population affects the law of change in that population when the population density is low, W. Allee proposed the famous Allee effect [9]. If the population density is too sparse, then mating between populations becomes difficult, and Allee effects may occur when the population density is under a specific threshold. Thus, Allee effects are strongly related to the vulnerability of populations to extinction [10–12]. For example, if pressure from the harvesting of bluefin tuna (*Thunnus thynnus*) is too strong, the population will collapse [11]. At a very small population size, the probability of finding an acceptable mate for some endangered species, such as lakapo (*Strigos habroptilus*), is very low [11].

The earliest single-population model exhibiting the Allee effect is as follows [13]:

$$\frac{du(t)}{dt} = r_1 u(t) \left( 1 - \frac{u(t)}{K} \right) (u(t) - a_0),$$

where  $u(t)$  represents the density of prey at time  $t$ , and  $r_1$  and  $K$  are the prey’s intrinsic growth rate and carrying capacity, respectively. The parameter  $a_0$  denotes the Allee threshold, and the term  $(u(t) - a_0)$  denotes the Allee effect. It must be noted that the Allee threshold is the critical population size or density below which the per capita population growth rate becomes negative. A strong Allee effect is an Allee effect at the Allee threshold. Whether the Allee effect is weak or strong depends on the opposing strengths of positive and negative density dependence. After the introduction of this model, many researchers began to pay attention to predator–prey models with strong Allee effects.

In nature, the influence of predators on prey species is not mediated only by simple predatory behavior. Since the prey has memory, the presence of predators has an inevitable impact on the behavior and psychology of the prey. For example, when a predator appears, the prey will be vigilant and will stop eating and breeding. This indirect effect on prey populations is known as the fear effect, and it is found widely in nature. Many researchers have focused on predator–prey models with the fear effect [14–16]. However, these models describe the prey as having a fear effect in connection with the predator, which affects the growth law of the prey. In nature, predators also have fear effects. For example, scientists have used the barking of dogs on a tape to simulate a scene of fear in raccoons. In this way, raccoons reduce their frequency and time of foraging; this protects the raccoons’ prey to maintain a balance in the ecosystem. In [17], T. Liu et al. proposed a predator–prey model with a fear effect on the predator and a strong Allee effect on the prey:

$$\begin{cases} \frac{du(t)}{dt} = r_1 u(t) \left(1 - \frac{u(t)}{K}\right) (u(t) - a_0) - \frac{\lambda u(t)v(t)}{1 + kv(t)}, \\ \frac{dv(t)}{dt} = \frac{r_2 v(t)}{1 + kv(t)} \left(1 - \frac{v(t)}{qu(t)}\right). \end{cases} \tag{1}$$

where  $u(t)$  and  $v(t)$  represent the densities of the prey and predator, respectively; and  $r_1$ ,  $K$ ,  $a_0$ ,  $\lambda$ ,  $k$ ,  $r_2$ , and  $q$  are the prey’s intrinsic growth rate, the carrying capacity, the strong Allee effect, the capture rate, a measure of the fear effect, the predator’s intrinsic growth rate, and a measure of food quality for the predator, respectively. More explanations of the parameters can be found in [17]. By setting  $\tilde{u} = \frac{u}{K}$ ,  $\tilde{v} = \frac{v}{Kq}$ ,  $\tilde{t} = \frac{t}{Kr_1}$ ,  $a = \frac{a_0}{K}$ ,  $c = \frac{\lambda q K}{r_1}$ ,  $s = kqK$ , and  $r = \frac{r_2}{r_1 K}$  and dropping “~”, model (1) is changed into

$$\begin{cases} \frac{du(t)}{dt} = u(t) \left( (1 - u(t))(u(t) - a) - \frac{cv(t)}{1 + sv(t)} \right), \\ \frac{dv(t)}{dt} = \frac{rv(t)}{1 + sv(t)} \left( 1 - \frac{v(t)}{u(t)} \right). \end{cases} \tag{2}$$

The authors mainly studied model (2) from the perspective of bifurcation, such as Hopf bifurcation and Bogdanov–Takens bifurcation [17]. Research has shown that increasing the fear effect on the predator is conducive to protecting prey populations.

We assume that the concentration distribution of species is uniform in model (2), but this is not always the actual situation in nature. In real nature, due to widespread self-diffusion phenomena, few populations of species have a homogeneous spatial distribution [18–20]. This is precisely because of the existence of diffusion phenomena; population models often show some more abundant dynamic phenomena, such as spatially inhomogeneous periodic solutions, spatial patterns, etc. In addition, time delays also exist [21–23], such as time delays in maturity, gestation, and predation. Time delays often affect the stability of the constant steady-state solution, and they cause periodic oscillations in the population density. Therefore, we introduce self-diffusion and time delay into model (2) as follows.

$$\begin{cases} \frac{\partial u(x, t)}{\partial t} = d_1 \Delta u(x, t) + u(x, t) \left( (1 - u(x, t))(u(x, t) - a) - \frac{cv(x, t)}{1 + sv(x, t)} \right), \\ \frac{\partial v(x, t)}{\partial t} = d_2 \Delta v(x, t) + \frac{rv(x, t)}{1 + sv(x, t)} \left( 1 - \frac{v(x, t - \tau)}{u(x, t - \tau)} \right). \end{cases} \tag{3}$$

where  $d_1, d_2 > 0$  represent the self-diffusion coefficients of the prey and predator, respectively, and  $\tau$  is the gestation delay in the predator. The growth law of the predator (the second equation in (3)) can be considered a logistic growth law, where  $(u(t - \tau))$  is the carrying capacity of the environment. An increase in density of predators at time  $t$  already exists for predators at time  $t - \tau$ , where  $\tau$  is the gestation time of predators. Therefore, the negative feedback of the density of the predator at time  $t$  is related to the relationship between the predator and the prey at time  $t - \tau$ .

In nature, animals in the same area usually compete for a common but limited resource; due to the depletion of resources, intraspecies competition effects should depend on the average population density in the neighborhood of the current location. In [24,25], the author suggested that internal competition within the population is often spatially inhomogeneous and measured this effect by weighting and integration, modifying the  $\frac{u}{K}$  as  $\frac{1}{K} \int_{\Omega} G(x, y)u(y, t)dy$ .  $G(x, y)$  is a kernel function. In [26], Geng et al. studied Hopf, Turing, double-Hopf, and Turing–Hopf bifurcations of a diffusive predator–prey model with nonlocal competition. In [27], Liu et al. studied a diffusive predator–prey model with nonlocal competition and time delay. These works show that spatially inhomogeneous bifurcating periodic solutions are stable, in contrast to models without nonlocal competition. A predator–prey model with nonlocal competition can produce complex dynamics, such as spatiotemporal patterns and stably spatially inhomogeneous periodic solutions [26–29].

Based on the above considerations, we introduce nonlocal competition among prey into model (3) as follows.

$$\begin{cases} \frac{\partial u(x, t)}{\partial t} = d_1 \Delta u(x, t) + u(x, t) \left( \left( 1 - \int_{\Omega} G(x, y)u(y, t)dy \right) (u(x, t) - a) - \frac{cv(x, t)}{1 + sv(x, t)} \right), \\ \frac{\partial v(x, t)}{\partial t} = d_2 \Delta v(x, t) + \frac{rv(x, t)}{1 + sv(x, t)} \left( 1 - \frac{v(x, t - \tau)}{u(x, t - \tau)} \right), \quad x \in \Omega, t > 0 \\ \frac{\partial u(x, t)}{\partial \bar{v}} = \frac{\partial v(x, t)}{\partial \bar{v}} = 0, \quad x \in \partial\Omega, t > 0 \\ u(x, \theta) = u_0(x, \theta) \geq 0, v(x, \theta) = v_0(x, \theta) \geq 0, \quad x \in \bar{\Omega}, \theta \in [-\tau, 0]. \end{cases} \tag{4}$$

The integral term  $\int_{\Omega} G(x, y)u(y, t)dy$  in the first equation of (4) accounts for nonlocal competition among the prey individuals. The kernel function is of the following form:

$$G(x, y) = \frac{1}{|\Omega|} = \frac{1}{l\pi}, \quad x, y \in \Omega,$$

which can be regarded as a measurement of the competition pressure at location  $x$  from the individuals at another location ( $y$ ), which is widely used by some scholars [26–28]. The region  $\Omega = (0, l\pi)$  with  $l > 0$  is used for the convenience of calculation. In this case, the strength of the competition among all prey individuals is the same across the habitat.

The aim of this paper is to consider the dynamics of model (4) from the perspective of stability and Hopf bifurcation and to study the effects of the Allee effect and fear effect on population growth law using numerical simulation. This article is structured as follows. In Section 2, we analyze the stability of the coexisting equilibrium and the existence of Hopf bifurcation. In Section 3, we analyze the properties of Hopf bifurcation. In Section 4, we perform some numerical simulations and analyze the results. In Section 5, we provide a brief conclusion.

### 2. Stability Analysis

In [17], the authors found that system (4) had no less than one equilibrium, which was noted as  $E_*(u_*, v_*)$ . We can obtain the concrete form of  $u_*$  by calculating the positive root of the following equation:

$$su^3 - (as + s - 1)u^2 + (as + c - a - 1)u + a = 0 = 0. \tag{5}$$

For the completeness of the article, we provide the following lemma and a numerical simulation (see Figure 1). In Figure 1, we can see that with the increase in parameter  $a$ , the two positive equilibrium points degenerate into one positive equilibrium point. However, when parameter  $a$  is greater than a certain critical value, the positive equilibrium point disappears.

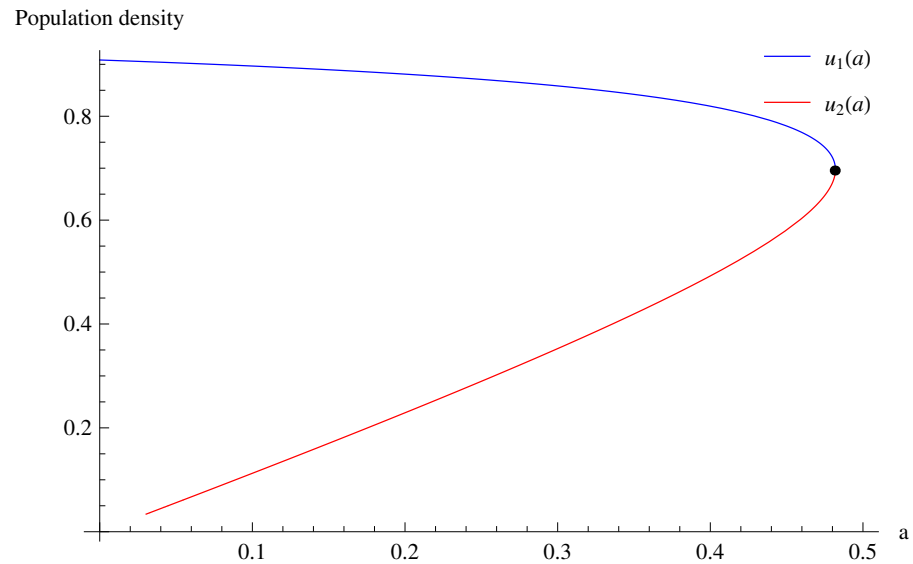


**Figure 1.** Positive roots of (5) with  $a$  under the following parameter settings:  $s = 0.1, c = 0.1,$  and  $r = 0.25$ .

**Lemma 1.** *If support  $(H_1)$  holds, the following results are true for system (4).*

1. *If  $c < a(1 - s)$  or  $c > a(1 - s) + 1, s(a + 1) > 1$ :*
  - (a). *If  $D < 0$ , there are two distinct positive equilibria;*
  - (b). *If  $D = 0$ ,*
    - (ib). *if  $A > 0$ , there exists a unique positive equilibrium;*
    - (iib). *if  $A = 0$ , there exists no positive equilibrium;*
  - (c). *If  $D > 0$ , there exists no positive equilibrium.*
2. *If  $c \geq a(1 - s), s(a + 1) \leq 1$ , there exists no positive equilibrium.*

$$\begin{aligned}
 A &= (as + s - 1)^2 - 3s(as + c - a - 1), \\
 B &= -(as + s - 1)(as + c - a - 1) - 9as, \\
 C &= (as + c - a - 1)^2 + 3a(as + s - 1), \\
 D &= -B^2 - 4AC.
 \end{aligned} \tag{6}$$

According to [17],  $(u_2, v_2)$  is always the saddle point under this set of parameters. We mainly study the stability and Hopf bifurcation of the equilibrium  $((u_1, v_1))$  in the following. We linearize system (4) at  $E_*(u_*, v_*)$ :

$$\frac{\partial}{\partial t} \begin{pmatrix} u(x, t) \\ u(x, t) \end{pmatrix} = D \begin{pmatrix} \Delta u(x, t) \\ \Delta v(x, t) \end{pmatrix} + L_1 \begin{pmatrix} u(x, t) \\ v(x, t) \end{pmatrix} + L_2 \begin{pmatrix} u(x, t - \tau) \\ v(x, t - \tau) \end{pmatrix} + L_3 \begin{pmatrix} \hat{u}(x, t) \\ \hat{v}(x, t) \end{pmatrix}, \tag{7}$$

where

$$\begin{aligned}
 D &= \begin{pmatrix} d_1 & 0 \\ 0 & d_2 \end{pmatrix}, \quad L_1 = \begin{pmatrix} a_1 & a_2 \\ 0 & 0 \end{pmatrix}, \quad L_2 = \begin{pmatrix} 0 & 0 \\ b_1 & -b_1 \end{pmatrix}, \quad L_3 = \begin{pmatrix} \hat{a} & 0 \\ 0 & 0 \end{pmatrix}, \\
 a_1 &= (1 - u_*)u_* > 0, \quad a_2 = -\frac{cu_*}{(1 + su_*)^2} < 0, \quad b_1 = \frac{r}{1 + su_*} > 0, \quad \hat{a} = -u_*(u_* - a) < 0,
 \end{aligned} \tag{8}$$

and  $\hat{u} = \frac{1}{l\pi} \int_0^{l\pi} u(y, t) dy$ .

Then, the characteristic equations of (7) are

$$\lambda^2 + P_n \lambda + Q_n + (R_n + b_1 \lambda) e^{-\lambda \tau} = 0, \quad n \in \mathbb{N}_0, \tag{9}$$

where

$$\begin{aligned} P_0 &= -\hat{a} - a_1, \quad Q_0 = 0, \quad R_0 = -(\hat{a} + a_1 + a_2) b_1, \\ P_n &= (d_1 + d_2) \frac{n^2}{l^2} - a_1, \quad Q_n = d_2 \frac{n^2}{l^2} \left( d_1 \frac{n^2}{l^2} - a_1 \right), \\ R_n &= b_1 \left( d_1 \frac{n^2}{l^2} - (a_1 + a_2) \right), \quad n \in \mathbb{N}. \end{aligned} \tag{10}$$

Let  $\tau = 0$ ; Equation (9) becomes

$$\lambda^2 + (P_n + b_1) \lambda + Q_n + R_n = 0, \quad n \in \mathbb{N}_0. \tag{11}$$

We make the following hypothesis:

$$(\mathbf{H}_1) \quad P_n + b_1 > 0, \quad Q_n + R_n > 0, \quad \text{for } n \in \mathbb{N}_0.$$

Under this hypothesis  $(\mathbf{H}_1)$ ,  $E_*(u_*, v_*)$  is locally asymptotically stable when  $\tau = 0$ . Next, we will discuss the case of  $\tau > 0$ .

**Lemma 2.** *If support  $(\mathbf{H}_1)$  holds, the following results are true for Equation (9):*

1. *There exists a pair of purely imaginary roots:  $\pm i\omega_n^\pm$  at  $\tau_n^{j,\pm}$  for  $j \in \mathbb{N}_0$  and  $n \in \mathbb{W}_1$ ;*
2. *There are two pairs of purely imaginary roots:  $\pm i\omega_n^\pm$  at  $\tau_n^{j,\pm}$  for  $j \in \mathbb{N}_0$  and  $n \in \mathbb{W}_2$ ;*
3. *There exists no purely imaginary root for  $n \in \mathbb{W}_3$ ,*

where  $\pm i\omega_n^\pm, \tau_n^{j,\pm}, \mathbb{W}_1, \mathbb{W}_2$ , and  $\mathbb{W}_3$  are defined in (14) and (15).

**Proof.** Let  $i\omega$  ( $\omega > 0$ ) be a solution of Equation (9). Then,

$$-\omega^2 + i\omega P_n + Q_n + (R_n + b_1 i\omega)(\cos\omega\tau - i\sin\omega\tau) = 0, \quad n \in \mathbb{N}_0.$$

Obviously,  $\cos\omega\tau = \frac{\omega^2(R_n - b_1 P_n) - Q_n R_n}{R_n^2 + b_1^2 \omega^2}$ ,  $\sin\omega\tau = \frac{\omega(P_n R_n - b_1(\omega^2 - Q_n))}{R_n^2 + b_1^2 \omega^2}$ . This leads to

$$\omega^4 + \omega^2 (P_n^2 - 2Q_n - b_1^2) + Q_n^2 - R_n^2 = 0, \quad n \in \mathbb{N}_0. \tag{12}$$

Let  $z = \omega^2$ ; then, (12) becomes

$$z^2 + z (P_n^2 - 2Q_n - b_1^2) + Q_n^2 - R_n^2 = 0, \quad n \in \mathbb{N}_0. \tag{13}$$

Let  $H_n = P_n^2 - 2Q_n - b_1^2$ ,  $J_n = Q_n + R_n$ , and  $K_n = Q_n - R_n$ . Then,  $z^\pm = \frac{1}{2}[-H_n \pm \sqrt{H_n^2 - 4J_n K_n}]$  are the roots of (13). If  $(\mathbf{H}_1)$  holds,  $J_n > 0$  ( $n \in \mathbb{N}_0$ ). Then, we can obtain

$$\begin{aligned} H_0 &= (\hat{a} + a_1)^2 - b_1^2, \\ H_k &= \left( a_1 - d_1 \frac{k^2}{l^2} \right)^2 + d_2^2 \frac{k^4}{l^4} - b_1^2, \quad \text{for } k \in \mathbb{N} \\ K_0 &= b_1(\hat{a} + a_1 + a_2) < 0, \\ K_k &= d_1 d_2 \frac{k^4}{l^4} - (b_1 d_1 + a_1 d_2) \frac{k^2}{l^2} + (a_1 + a_2) b_1, \quad \text{for } k \in \mathbb{N}. \end{aligned}$$

We define

$$\begin{aligned} \mathbb{S}_1 &= \{n | K_n < 0, n \in \mathbb{N}_0\}, \\ \mathbb{S}_2 &= \{n | K_n > 0, H_n < 0, H_n^2 - 4J_nK_n > 0, n \in \mathbb{N}\}, \\ \mathbb{S}_3 &= \{n | K_n > 0, H_n^2 - 4J_nK_n < 0, n \in \mathbb{N}\}, \end{aligned} \tag{14}$$

and

$$\begin{aligned} \omega_n^\pm &= \sqrt{z_n^\pm}, \quad \tau_n^{j,\pm} = \begin{cases} \frac{1}{\omega_n^\pm} \arccos(V_{\cos}^{(n,\pm)}) + 2j\pi, & V_{\sin}^{(n,\pm)} \geq 0, \\ \frac{1}{\omega_n^\pm} [2\pi - \arccos(V_{\cos}^{(n,\pm)})] + 2j\pi, & V_{\sin}^{(n,\pm)} < 0. \end{cases} \\ V_{\cos}^{(n,\pm)} &= \frac{(\omega_n^\pm)^2(b_2P_n + R_n) - M_nR_n}{R_n^2 + b_1^2(\omega_n^\pm)^2}, \quad V_{\sin}^{(n,\pm)} = \frac{\omega_n^\pm(P_nR_n + Q_nb_2 + b_1(\omega_n^\pm)^2)}{R_n^2 + b_1^2(\omega_n^\pm)^2}. \end{aligned} \tag{15}$$

It is easy to verify the conclusion in Lemma 2. □

**Lemma 3.** Support  $(H_1)$  is satisfied. Then,  $Re(\frac{d\lambda}{d\tau})|_{\tau=\tau_n^{j,+}} > 0$ ,  $Re(\frac{d\lambda}{d\tau})|_{\tau=\tau_n^{j,-}} < 0$  for  $n \in \mathbb{S}_1 \cup \mathbb{S}_2$  and  $j \in \mathbb{N}_0$ .

**Proof.** According to (9), we have

$$\left(\frac{d\lambda}{d\tau}\right)^{-1} = \frac{2\lambda + P_n + b_1e^{-\lambda\tau}}{(R_n + b_1\lambda)\lambda e^{-\lambda\tau}} - \frac{\tau}{\lambda}.$$

Then,

$$\begin{aligned} [Re(\frac{d\lambda}{d\tau})^{-1}]_{\tau=\tau_n^{j,\pm}} &= Re[\frac{2\lambda + P_n + b_1e^{-\lambda\tau}}{(R_n + b_1\lambda)\lambda e^{-\lambda\tau}} - \frac{\tau}{\lambda}]_{\tau=\tau_n^{j,\pm}} \\ &= [\frac{1}{R_n^2 + b_1^2\omega^2}(2\omega^2 + P_n^2 - 2Q_n - b_1^2)]_{\tau=\tau_n^{j,\pm}} \\ &= \pm[\frac{1}{R_n^2 + b_1^2\omega^2}\sqrt{(P_n^2 - 2Q_n - b_1^2)^2 - 4(Q_n^2 - R_n^2)}]_{\tau=\tau_n^{j,\pm}}. \end{aligned}$$

Therefore,  $Re(\frac{d\lambda}{d\tau})|_{\tau=\tau_n^{j,+}} > 0$ ,  $Re(\frac{d\lambda}{d\tau})|_{\tau=\tau_n^{j,-}} < 0$ . □

We denote  $\tau_* = \min\{\tau_n^0 | n \in \mathbb{S}_1 \cup \mathbb{S}_2\}$ .

Naturally, we have the following theorem.

**Theorem 1.** Assume that  $(H_1)$  holds; then, the following statements are true for system (4).

1.  $E_*(u_*, v_*)$  is locally asymptotically stable for  $\tau > 0$  when  $\mathbb{S}_1 \cup \mathbb{S}_2 = \emptyset$ ;
2.  $E_*(u_*, v_*)$  is locally asymptotically stable for  $\tau \in [0, \tau_*)$  when  $\mathbb{S}_1 \cup \mathbb{S}_2 \neq \emptyset$ ;
3.  $E_*(u_*, v_*)$  is unstable for  $\tau \in (\tau_*, \tau_* + \varepsilon)$  for some  $\varepsilon > 0$  when  $\mathbb{S}_1 \cup \mathbb{S}_2 \neq \emptyset$ ;
4. Hopf bifurcation occurs at  $(u_*, v_*)$  when  $\tau = \tau_n^{j,+}$  ( $\tau = \tau_n^{j,-}$ ),  $j \in \mathbb{N}_0, n \in \mathbb{S}_1 \cup \mathbb{S}_2$ .

Because stability switching is a highly concerned dynamic phenomenon [30–32], we provide the following remark about stability switching.

**Remark 1.** According to lemma 3, we know that  $Re(\frac{d\lambda}{d\tau})|_{\tau=\tau_n^{j,+}} > 0$ ,  $Re(\frac{d\lambda}{d\tau})|_{\tau=\tau_n^{j,-}} < 0$ . If  $\mathbb{W}_2 \neq \emptyset$  and there exist  $\tau_* = \tau_{n_1}^{0,+} < \tau_{n_1}^{0,-}$ ,  $\tau_* = \tau_{n_1}^{0,+} < \tau_{n_2}^{0,+} < \tau_{n_2}^{0,-} < \tau_{n_1}^{0,-}$ ,  $\tau_* = \tau_{n_1}^{0,+} < \tau_{n_2}^{0,+} < \dots < \tau_{n_j}^{0,+} < \tau_{n_j}^{0,-} < \dots < \tau_{n_2}^{0,-} < \tau_{n_1}^{0,-}$ , or other alternating forms of  $\tau_n^{j,\pm}$ . Then, stability switching may exist.

### 3. Properties of Hopf Bifurcation

From [33,34], we learned how to analyze the properties of Hopf bifurcation. For fixed  $j \in \mathbb{N}_0$  and  $n \in \mathbb{S}_1 \cup \mathbb{S}_2$ , we define  $\tilde{\tau} = \tau_n^{j,\pm}$ . Let  $\bar{u}(x, t) = u(x, \tau t) - u_*$  and  $\bar{v}(x, t) = v(x, \tau t) - v_*$ . By ignoring the bar, (4) becomes

$$\begin{cases} \frac{\partial u}{\partial t} = \tau[d_1\Delta u + (u + u_*)\left(1 - \frac{1}{l\pi} \int_0^{l\pi} (u(y, t) + u_*)dy\right)(u + u_* - a) - \frac{c(v + v_*)}{1 + s(v + v_*)}], \\ \frac{\partial v}{\partial t} = \tau[d_2\Delta v + \frac{r(v + v_*)}{1 + s(v + v_*)}\left(1 - \frac{v(t-1) + v_*}{u(t-1) + u_*}\right)]. \end{cases} \tag{16}$$

Then, we rewrite (16) in the following form:

$$\begin{cases} \frac{\partial u}{\partial t} = \tau[d_1\Delta u + a_1u + a_2v - \hat{a}u + \alpha_1u^2 + (a - 2u_*)u\bar{u} + \alpha_2u\bar{v} + \alpha_3v^2 + \alpha_4u\bar{v}^2 + \alpha_5\bar{v}^3] + h.o.t., \\ \frac{\partial v}{\partial t} = \tau[d_2\Delta v - \eta\sigma v + b_1u(t-1) - b_1v(t-1) + \beta_1u^2(t-1) + \beta_2u(t-1)v + \beta_3u(t-1)v(t-1) + \beta_4v\bar{v}(t-1) \\ + \beta_5u^3(t-1) + \beta_6u^2(t-1)v + \beta_7u(t-1)v^2 + \beta_8u^2(t-1)v(t-1)] + h.o.t., \end{cases} \tag{17}$$

where  $\alpha_1 = 1 - u_*$ ,  $\alpha_2 = -\frac{c}{(1+su_*)^2}$ ,  $\alpha_3 = \frac{csu_*}{(1+su_*)^3}$ ,  $\alpha_4 = \frac{cs}{(1+su_*)^3}$ ,  $\alpha_5 = -\frac{cs^2u_*}{(1+su_*)^4}$ ,  $\beta_1 = -\frac{r}{u_*(1+su_*)}$ ,  $\beta_2 = \frac{r}{u_*(1+su_*)^2}$ ,  $\beta_3 = \frac{r}{u_*(1+su_*)}$ ,  $\beta_4 = -\frac{r}{u_*(1+su_*)^2}$ ,  $\beta_5 = \frac{r}{u_*^2(1+su_*)}$ ,  $\beta_6 = -\frac{r}{u_*^2(1+su_*)^2}$ ,  $\beta_7 = -\frac{rs}{u_*(1+su_*)^3}$ , and  $\beta_8 = -\frac{r}{u_*^2(1+su_*)}$ .

We define a space,  $X := \{(u, v)^T : u, v \in H^2(0, l\pi), (u_x, v_x)|_{x=0, l\pi} = 0\}$ , which is called real-valued Sobolev.  $X_{\mathbb{C}}$  is the complexification of  $X$ , which has the form  $X_{\mathbb{C}} := X \oplus iX = \{u + iv | u, v \in X\}$ . Then, we define the inner product:  $\langle \tilde{u}, \tilde{v} \rangle := \int_0^{l\pi} \bar{u}_1v_1dx + \int_0^{l\pi} \bar{u}_2v_2dx$ , where  $\tilde{u} = (u_1, u_2)^T \in X_{\mathbb{C}}$ ,  $\tilde{v} = (v_1, v_2)^T \in X_{\mathbb{C}}$ .

We define the phase space,  $\mathcal{C} := C([-1, 0], X)$ , which is with the sup norm. Then, we have  $\varphi_t \in \mathcal{C}$ ,  $\varphi_t(\sigma) = \varphi(t + \sigma)$  for  $\sigma \in [-1, 0]$ . To define the subspace of  $\mathcal{C}$ , we made the following definitions:  $\alpha_n^{(1)}(u) = (\gamma_n(u), 0)^T$ ,  $\alpha_n^{(2)}(u) = (0, \gamma_n(u))^T$ , and  $\alpha_n = \{\alpha_n^{(1)}(u), \alpha_n^{(2)}(u)\}$ , where  $\{\alpha_n^{(i)}(u)\}$  is an orthonormal basis of  $X$ . Then, we define the subspace of  $\mathcal{C}$  as  $\mathbb{B}_n := \text{span}\{\langle \varphi(\cdot), \alpha_n^{(j)} \rangle \alpha_n^{(j)} | \varphi \in \mathcal{C}, j = 1, 2, n \in \mathbb{N}_0\}$ . For  $\theta \in [-1, 0]$  and  $\varphi \in \mathcal{C}$ , the  $2 \times 2$  matrix function  $(\eta^n(\theta, \tilde{\tau}))$  can satisfy the following:  $-\tilde{\tau}D\frac{\eta^2}{l^2}\varphi(0) + \tilde{\tau}L(\varphi) = \int_{-1}^0 d\eta^n(\theta, \tau)\varphi(\theta)$ . Then, Equation (18) defines the bilinear form on  $\mathcal{C}^* \times \mathcal{C}$  for  $\psi \in \mathcal{C}^*$ ,  $\phi \in \mathcal{C}$ .

$$(\phi, \psi) = \phi(0)\psi(0) - \int_{-1}^0 \int_{\tilde{\xi}=0}^{\theta} \phi(\tilde{\xi} - \theta)d\eta^n(\theta, \tilde{\tau})\psi(\tilde{\xi})d\tilde{\xi}, \tag{18}$$

Let  $\tau = \tilde{\tau} + \mu$ . When  $\mu = 0$ , the characteristic equation of the system has a pair of purely imaginary roots  $(\pm i\omega_{n_0})$ , and the system undergoes Hopf bifurcation at  $(0, 0)$ . Assume that  $A$  represents the infinitesimal generators of the semigroup, and  $A^*$  represents the formal adjoint of  $A$  under the bilinear form (18).

We define

$$\delta(n_0) = \begin{cases} 1 & n_0 = 0, \\ 0 & n_0 \in \mathbb{N}. \end{cases} \tag{19}$$

Let  $\eta_{n_0}(0, \tilde{\tau}) = \tilde{\tau}[(-n_0^2/l^2)D + L_1 + L_3\delta(n_{n_0})]$ ,  $\eta_{n_0}(-1, \tilde{\tau}) = -\tilde{\tau}L_2$ , and  $\eta_{n_0}(\sigma, \tilde{\tau}) = 0$  for  $\sigma \in [-1, 0]$ . We define  $p(\theta) = p(0)e^{i\omega_{n_0}\tilde{\tau}\theta}$  ( $\theta \in [-1, 0]$ ) as the eigenfunction of  $A(\tilde{\tau})$  for  $i\omega_{n_0}\tilde{\tau}$ , and  $q(\vartheta) = q(0)e^{-i\omega_{n_0}\tilde{\tau}\vartheta}$  ( $\vartheta \in [0, 1]$ ) is the eigenfunction of  $A^*$  for  $i\omega_{n_0}\tilde{\tau}$ . Let

$p(0) = (1, p_1)^T, q(0) = M(1, q_2)$ , where  $p_1 = \frac{1}{a_2}(i\omega_{n_0} + d_1 n_0^2 / l^2 - a_1 - \hat{a}\delta(n_0))$ ,  $q_2 = \frac{a_2}{i\omega_{n_0} + b_1 e^{i\omega_{n_0} + d_2 n^2 / l^2}}$ , and  $M = (1 + p_1 q_2 + \tilde{\tau} q_2 b_1 (1 - p_1) e^{-i\omega_{n_0} \tilde{\tau}})^{-1}$ . Then, (16) becomes

$$\frac{dU(t)}{dt} = (\tilde{\tau} + \mu) D\Delta U(t) + (\tilde{\tau} + \mu) [L_1 U(t) + L_2 U(t - 1) + L_3 \hat{U}(t)] + F(\mu, U_t, \hat{U}_t), \tag{20}$$

where

$$F(\phi, \mu) = (\tilde{\tau} + \mu) \begin{pmatrix} \alpha_1 \phi_1(0)^2 - (2u_* - \beta) \phi_1(0) \hat{\phi}_1(0) + \alpha_2 \phi_1(0) \phi_2(0) + \alpha_3 \phi_2(0)^2 + \alpha_4 \phi_1^3(0) \\ \quad + \alpha_5 \phi_1^2(0) \phi_2(0) + \alpha_6 \phi_1(0) \phi_2^2(0) + \alpha_7 \phi_2^3(0) \\ \beta_1 \phi_1^2(-1) + \beta_2 \phi_1(-1) \phi_2(-1) + \beta_3 \phi_2^2(-1) + \beta_4 \phi_1^3(-1) + \beta_4 \phi_1^2(-1) \phi_2(-1) \\ \quad + \beta_6 \phi_1(-1) \phi_2^2(-1) + \beta_7 \phi_2^3(-1) \end{pmatrix} \tag{21}$$

for  $\phi = (\phi_1, \phi_2)^T \in \mathcal{C}$  and  $\hat{\phi}_1 = \frac{1}{l\pi} \int_0^{l\pi} \phi dx$ . Then, we decompose the space ( $\mathcal{C}$ ) as  $\mathcal{C} = P \oplus Q$ , where  $P = \{z p \gamma_{n_0}(x) + \bar{z} \bar{p} \gamma_{n_0}(x) | z \in \mathbb{C}\}$ ,  $Q = \{\phi \in \mathcal{C} | (q \gamma_{n_0}(x), \phi) = 0, \text{ and } (\bar{q} \gamma_{n_0}(x), \phi) = 0\}$ . Then, (21) is rewritten as  $U_t = z(t) p(\cdot) \gamma_{n_0}(x) + \bar{z}(t) \bar{p}(\cdot) \gamma_{n_0}(x) + \omega(t, \cdot)$ , and  $\hat{U}_t = \frac{1}{l\pi} \int_0^{l\pi} U_t dx$ , where

$$z(t) = (q \gamma_{n_0}(x), U_t), \quad \omega(t, \theta) = U_t(\theta) - 2\text{Re}\{z(t) p(\theta) \gamma_{n_0}(x)\}. \tag{22}$$

We found that  $\dot{z}(t) = i\omega_{n_0} \tilde{\tau} z(t) + \bar{q}(0) < F(0, U_t), \beta_{n_0} >$ . Then,  $\mathcal{C}_0$  and  $\omega$  can have the following form near  $(0, 0)$ :

$$\omega(t, \theta) = \omega(z(t), \bar{z}(t), \theta) = \omega_{20}(\theta) \frac{z^2}{2} + \omega_{11}(\theta) z\bar{z} + \omega_{02}(\theta) \frac{\bar{z}^2}{2} + \dots \tag{23}$$

We restrict the system to  $\mathcal{C}_0$  such that  $\dot{z}(t) = i\omega_{n_0} \tilde{\tau} z(t) + g(z, \bar{z})$ . Let  $g(z, \bar{z}) = g_{20} \frac{z^2}{2} + g_{11} z\bar{z} + g_{02} \frac{\bar{z}^2}{2} + g_{21} \frac{z^2 \bar{z}}{2} + \dots$ . By direct computation, we have

$$g_{20} = 2\tilde{\tau} M(\zeta_1 + q_2 \zeta_2) I_3, \quad g_{11} = \tilde{\tau} M(q_1 + q_2 q_2) I_3, \quad g_{02} = \bar{g}_{20},$$

$$g_{21} = 2\tilde{\tau} M[(\kappa_{11} + q_2 \kappa_{21}) I_2 + (\kappa_{12} + q_2 \kappa_{22}) I_4],$$

where  $I_2 = \int_0^{l\pi} \gamma_{n_0}^2(x) dx, I_3 = \int_0^{l\pi} \gamma_{n_0}^3(x) dx, I_4 = \int_0^{l\pi} \gamma_{n_0}^4(x) dx, \zeta_1 = (a - 2u_*) \delta_{n_0} + (\alpha_1 + p_1(\alpha_2 + \alpha_3 p_1)), \zeta_2 = e^{-2i\tau\omega_n} (\beta_1 + 2\beta_8 + e^{i\tau\omega_n} (\beta_2 + 2\beta_3 \beta_4) p_1), q_1 = \frac{1}{4} (2\alpha_1 + 2(a - 2u_*) \delta_{n_0} + 2\alpha_3 \bar{p}_1 p_1 + \alpha_2 (\bar{p}_1 + p_1)), q_2 = \frac{1}{4} e^{-i\tau\omega_n} (2e^{i\tau\omega_n} (\beta_1 + 2\beta_8) + (\beta_2 + 2\beta_3 \beta_4) \bar{p}_1 + e^{2i\tau\omega_n} (\beta_2 + 2\beta_3 \beta_4) p_1), \kappa_{11} = 2W_{11}^{(1)}(0)(2\alpha_1 + a(1 + \delta_{n_0}) - 2u_*(1 + \delta_{n_0}) + \alpha_2 p_1) + 2W_{11}^{(2)}(0)(\alpha_2 + 2\alpha_3 p_1) + W_{20}^{(1)}(0)(2\alpha_1 + a(1 + \delta_{n_0}) - 2u_*(1 + \delta_{n_0}) + \alpha_2 \bar{p}_1) + W_{20}^{(2)}(0)(\alpha_2 + 2\alpha_3 \bar{p}_1), \kappa_{12} = 2e^{-i\tau\omega_n} W_{11}^{(2)}(0)(\beta_2 + 2\beta_3 \beta_4) + e^{i\tau\omega_n} W_{20}^{(2)}(0)(\beta_2 + 2\beta_3 \beta_4) + 2e^{-i\tau\omega_n} W_{11}^{(1)}(-1)(2\beta_1 + 4\beta_8 + e^{i\tau\omega_n} (\beta_2 + 2\beta_3 \beta_4) p_1) + W_{20}^{(1)}(-1)(2e^{i\tau\omega_n} (\beta_1 + 2\beta_8) + (\beta_2 + 2\beta_3 \beta_4) \bar{p}_1), \kappa_{21} = \frac{1}{2} p_1 (3\alpha_5 \bar{p}_1 p_1 + \alpha_4 (2\bar{p}_1 + p_1)), \kappa_{22} = \frac{1}{2} e^{-2i\tau\omega_n} (e^{3i\tau\omega_n} \beta_7 p_1^2 + \bar{p}_1 (\beta_6 + 3\beta_3 \beta_4 p_1) + e^{i\tau\omega_n} (3\beta_5 + \beta_8 \bar{p}_1 + 2\beta_8 p_1 + 2\beta_7 \bar{p}_1 p_1) + e^{2i\tau\omega_n} p_1 (2\beta_6 + 3\beta_3 \beta_4 (\bar{p}_1 + p_1))).$

Next, for  $\theta \in [-1, 0]$ , we compute  $W_{20}$  and  $W_{11}$  to obtain  $g_{21}$ . According to (22), we have

$$\dot{\omega} = \dot{U}_t - \dot{z} p \gamma_{n_0}(x) - \dot{\bar{z}} \bar{p} \gamma_{n_0}(x) = A\omega + H(z, \bar{z}, \theta), \tag{24}$$

where

$$H(z, \bar{z}, \theta) = H_{20}(\theta) \frac{z^2}{2} + H_{11}(\theta) z\bar{z} + H_{02}(\theta) \frac{\bar{z}^2}{2} + \dots \tag{25}$$

By comparing the coefficients of (23) with those of (24), we have

$$(A - 2i\omega_{n_0} \tilde{\tau} I) \omega_{20} = -H_{20}(\theta), \quad A\omega_{11}(\theta) = -H_{11}(\theta). \tag{26}$$

Then, we have

$$\begin{aligned} \omega_{20}(\theta) &= \frac{-g_{20}}{i\omega_{n_0}\bar{\tau}}p(0)e^{i\omega_{n_0}\bar{\tau}\theta} - \frac{\bar{g}_{02}}{3i\omega_{n_0}\bar{\tau}}\bar{p}(0)e^{-i\omega_{n_0}\bar{\tau}\theta} + E_1e^{2i\omega_{n_0}\bar{\tau}\theta}, \\ \omega_{11}(\theta) &= \frac{g_{11}}{i\omega_{n_0}\bar{\tau}}p(0)e^{i\omega_{n_0}\bar{\tau}\theta} - \frac{\bar{g}_{11}}{i\omega_{n_0}\bar{\tau}}\bar{p}(0)e^{-i\omega_{n_0}\bar{\tau}\theta} + E_2, \end{aligned} \tag{27}$$

where  $E_1 = \sum_{n=0}^{\infty} E_1^{(n)}$ ,  $E_2 = \sum_{n=0}^{\infty} E_2^{(n)}$ ,

$$E_1^{(n)} = (2i\omega_{n_0}\bar{\tau}I - \int_{-1}^0 e^{2i\omega_{n_0}\bar{\tau}\theta} d\eta_{n_0}(\theta, \bar{\tau}))^{-1} \langle \tilde{F}_{20}, \beta_n \rangle,$$

$$E_2^{(n)} = -(\int_{-1}^0 d\eta_{n_0}(\theta, \bar{\tau}))^{-1} \langle \tilde{F}_{11}, \beta_n \rangle, \quad n \in \mathbb{N}_0,$$

$$\langle \tilde{F}_{20}, \beta_n \rangle = \begin{cases} \frac{1}{l\bar{\tau}}\hat{F}_{20}, & n_0 \neq 0, n = 0, \\ \frac{2}{2l\bar{\tau}}\hat{F}_{20}, & n_0 \neq 0, n = 2n_0, \\ \frac{1}{l\bar{\tau}}\hat{F}_{20}, & n_0 = 0, n = 0, \\ 0, & \text{other,} \end{cases} \quad \langle \tilde{F}_{11}, \beta_n \rangle = \begin{cases} \frac{1}{l\bar{\tau}}\hat{F}_{11}, & n_0 \neq 0, n = 0, \\ \frac{2}{2l\bar{\tau}}\hat{F}_{11}, & n_0 \neq 0, n = 2n_0, \\ \frac{1}{l\bar{\tau}}\hat{F}_{11}, & n_0 = 0, n = 0, \\ 0, & \text{other,} \end{cases}$$

and  $\hat{F}_{20} = 2(\zeta_1, \zeta_2)^T$ ,  $\hat{F}_{11} = 2(\varrho_1, \varrho_2)^T$ .

Thus, we can obtain

$$\begin{aligned} c_1(0) &= \frac{i}{2\omega_n\bar{\tau}}(g_{20}g_{11} - 2|g_{11}|^2 - \frac{|g_{02}|^2}{3}) + \frac{1}{2}g_{21}, \quad \mu_2 = -\frac{\text{Re}(c_1(0))}{\text{Re}(\lambda'(\bar{\tau}))}, \\ T_2 &= -\frac{1}{\omega_{n_0}\bar{\tau}}[\text{Im}(c_1(0)) + \mu_2\text{Im}(\lambda'(\tau_n^j))], \quad \beta_2 = 2\text{Re}(c_1(0)). \end{aligned} \tag{28}$$

**Theorem 2.** *The following results are true for any critical value  $(\tau_n^j (n \in \mathbb{S}, j \in \mathbb{N}_0))$ .*

1. *If  $\mu_2 > 0$  (or  $< 0$ ), the Hopf bifurcation is forward (or backward);*
2. *If  $\beta_2 < 0$  (or  $> 0$ ), the bifurcating periodic solutions on  $\mathcal{C}_0$  are orbitally asymptotically stable (or unstable);*
3. *If  $T_2 > 0$  (or  $T_2 < 0$ ), the period increases (or decreases).*

#### 4. Numerical Simulations

To analyze the influence of the fear effect parameter ( $s$ ), the strong Allee effect parameter ( $a$ ), and gestation delay ( $\tau$ ) on model (4), we performed the following numerical simulations. We fixed

$$c = 0.1, \quad r = 0.25, \quad d_1 = 0.5, \quad d_2 = 0.1, \quad l = 1.5.$$

The existence of a positive equilibrium is provided in Figure 1. Obviously, the equilibrium  $(u_2, v_2)$  is unstable through the following analysis, so we pay attention to the stability of the equilibrium  $(u_1, v_1)$ , which is positive. The bifurcation diagrams of model (4) with parameters  $s$  and  $a$  are provided in Figures 2 and 3, respectively. In Figure 2, we can observe that increasing parameter  $s$  can increase the stable region of the equilibrium and eliminate the periodic oscillation. In Figure 3, we find that increasing parameter  $a$  can decrease the stable region of the equilibrium and induce periodic oscillation.

If we choose  $a = 0.05$  and  $s = 0.1$ , then model (4) has two coexisting equilibria:  $(u_1, v_1) \approx (0.9029, 0.9029)$  and  $(u_2, v_2) \approx (0.0559, 0.0559)$ . By direct calculation, the hypothesis  $(H_1)$  holds for  $(u_1, v_1)$  and does not hold for  $(u_2, v_2)$ . Therefore, we mainly analyze the coexisting equilibrium  $(u_1, v_1)$ . By direct computation, we have  $\mathbb{S}_1 = \{0, 1, 2\}$  and  $\mathbb{S}_2 = \mathbb{S}_3 = \emptyset$ , as well as  $\tau_* = \tau_1^0 \approx 5.9478 < \tau_0^0 \approx 6.1053$ . Theorem 1 shows that the coexisting equilibrium  $(u_1, v_1)$  is locally asymptotically stable if  $\tau \in [0, \tau_*)$  (Figure 4). For model (4), Hopf bifurcation occurs if  $\tau = \tau_*$ . According to Theorem 2, we have

$$\mu_2 \approx 16.1916 > 0, \quad \beta_2 \approx -0.6295 < 0, \quad T_2 \approx 0.5672 > 0.$$

Therefore, when  $\tau > \tau_*$ , the bifurcating periodic solutions are stably spatially inhomogeneous (Figure 5). When we continue to increase parameter  $\tau$ , the bifurcating periodic solutions are still stably spatially inhomogeneous (Figure 6).

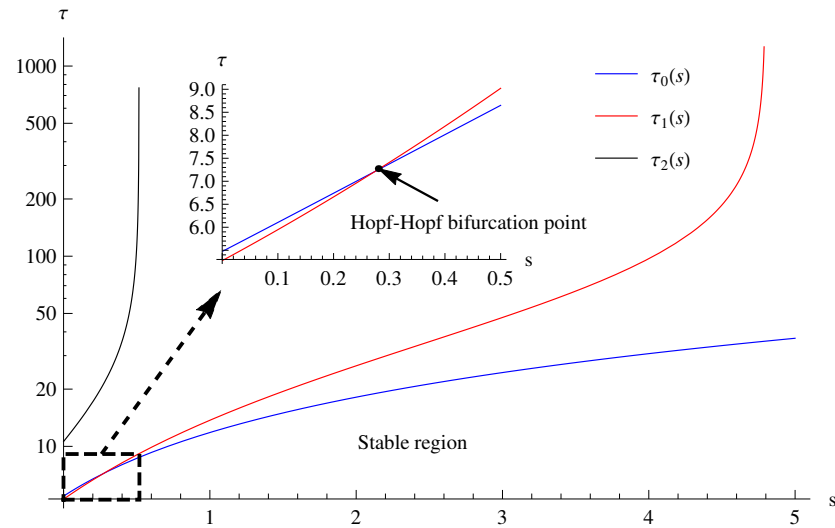


Figure 2. Bifurcation diagram for  $s$  and  $\tau$  with  $a = 0.05$  at the coexisting equilibrium  $(u_1, v_1)$ .

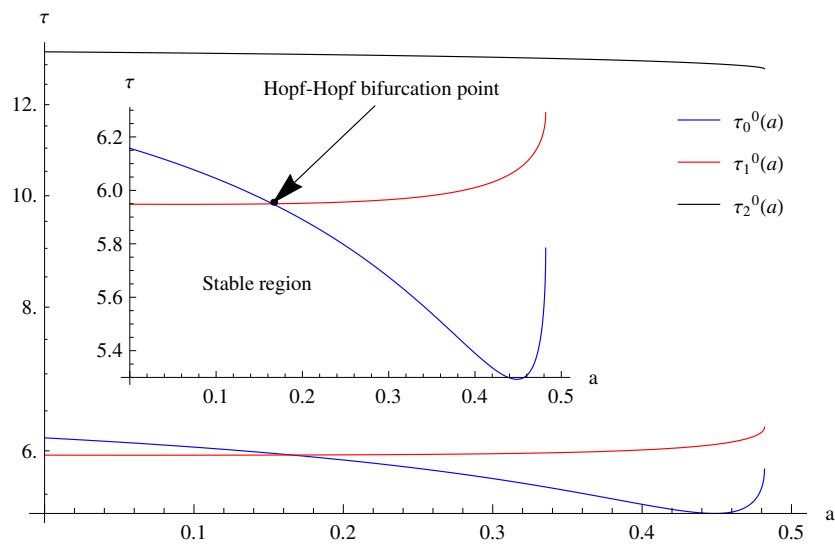


Figure 3. Bifurcation diagram for  $a$  and  $\tau$  with  $s = 0.1$  at the coexisting equilibrium  $(u_1, v_1)$ .

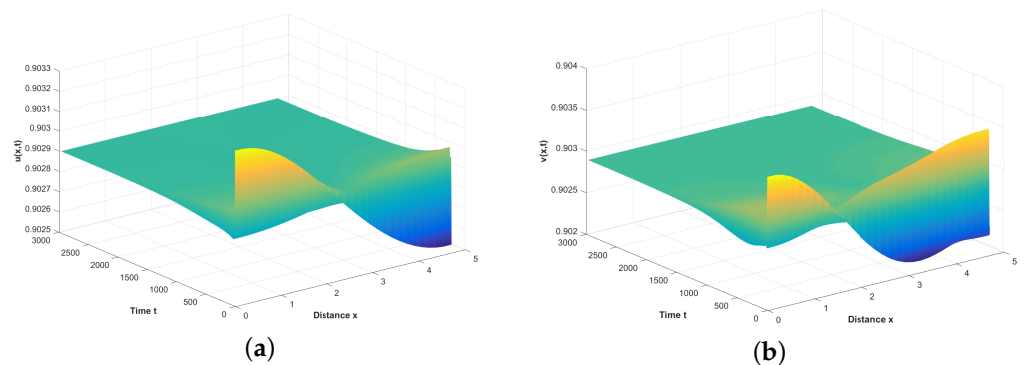
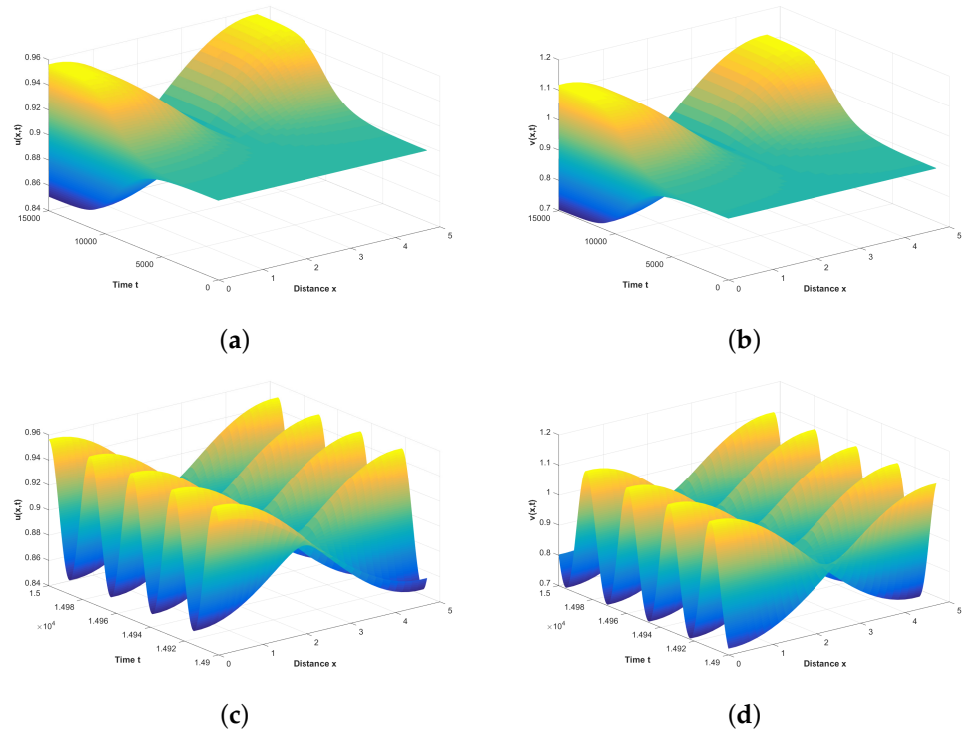
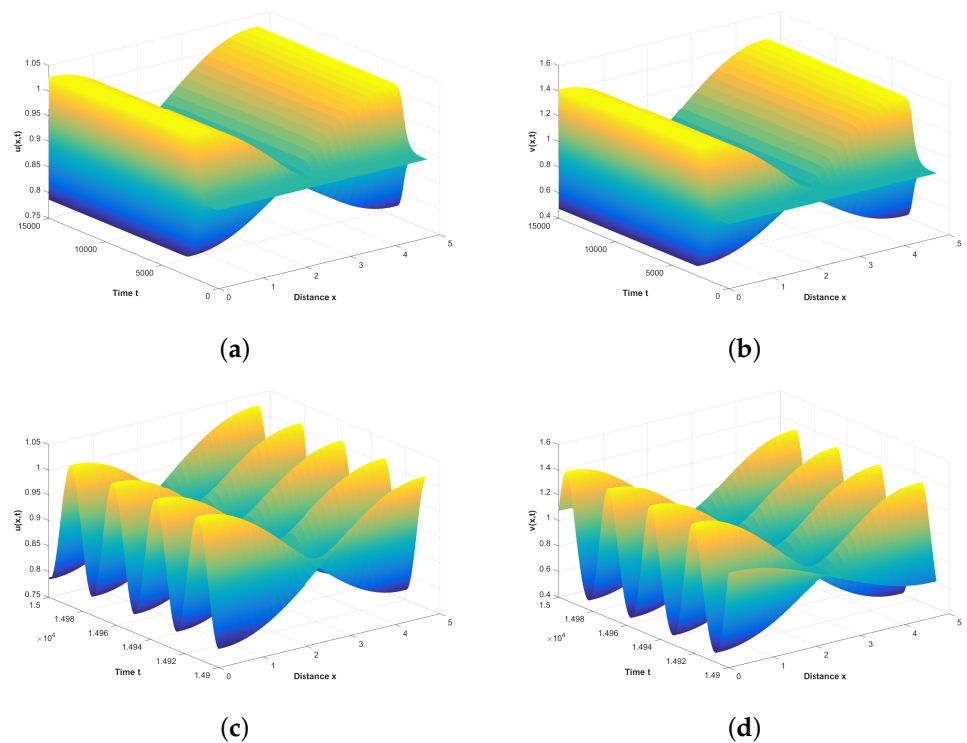


Figure 4. Numerical simulations for model (4) when  $\tau = 5.92 < \tau_1^0$  and for the initial values of  $u_0(x) = u_* + 0.001\cos x, v_0(x) = v_* - 0.001\cos x$ . (a) Prey. (b) Predator.



**Figure 5.** Numerical simulations for model (4) when  $\tau = 6.05 \in (\tau_1^0, \tau_0^0)$  and for the initial values of  $u_0(x) = u_* + 0.001\cos x, v_0(x) = v_* - 0.001\cos x$ . (a,c) Prey. (b,d) Predator.



**Figure 6.** Numerical simulations for model (4) when  $\tau = 6.2 > \tau_1^0$  and for the initial values of  $u_0(x) = u_* + 0.001\cos x, v_0(x) = v_* - 0.001\cos x$ . (a,c) Prey. (b,d) Predator.

If we choose  $a = 0.2$  and  $s = 0.1$ , then model (4) has two coexisting equilibria:  $(u_1, v_1) \approx (0.8811, 0.8811)$  and  $(u_2, v_2) \approx (0.2290, 0.2290)$ . By direct calculation, the hypothesis  $(H_1)$  holds for  $(u_1, v_1)$  and does not hold for  $(u_2, v_2)$ . Therefore, we mainly analyzed the coexisting equilibrium  $(u_1, v_1)$ . By direct computation, we have  $S_1 = \{0, 1, 2\}$

and  $\mathbb{S}_2 = \mathbb{S}_3 = \emptyset$ , as well as  $\tau_* = \tau_0^0 \approx 5.8910 < \tau_0^1 \approx 5.9517$ . Theorem 1 shows that the coexisting equilibrium  $(u_1, v_1)$  is locally asymptotically stable if  $\tau \in [0, \tau_*)$ . For model (4), Hopf bifurcation occurs if  $\tau = \tau_*$ . Theorem 2 shows that

$$\mu_2 \approx 43.8547 > 0, \beta_2 \approx -1.6464 < 0, T_2 \approx 10.3338 > 0.$$

Thus, when  $\tau > \tau_*$ , the bifurcating periodic solutions are stably spatially homogeneous (Figure 7). When we continue to increase parameter  $\tau$ , the bifurcating periodic solutions are still stably spatially homogeneous (Figure 8).

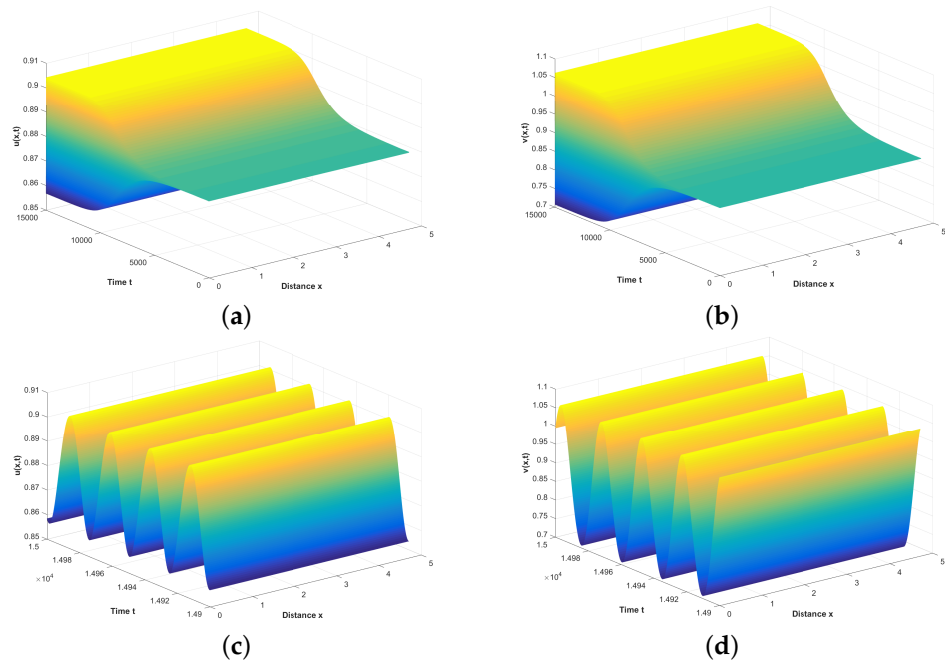


Figure 7. Numerical simulations for model (4) when  $\tau = 5.92 \in (\tau_0^0, \tau_0^1)$  and for the initial values of  $u_0(x) = u_* + 0.001\cos x, v_0(x) = v_* - 0.001\cos x$ . (a,c) Prey. (b,d) Predator.

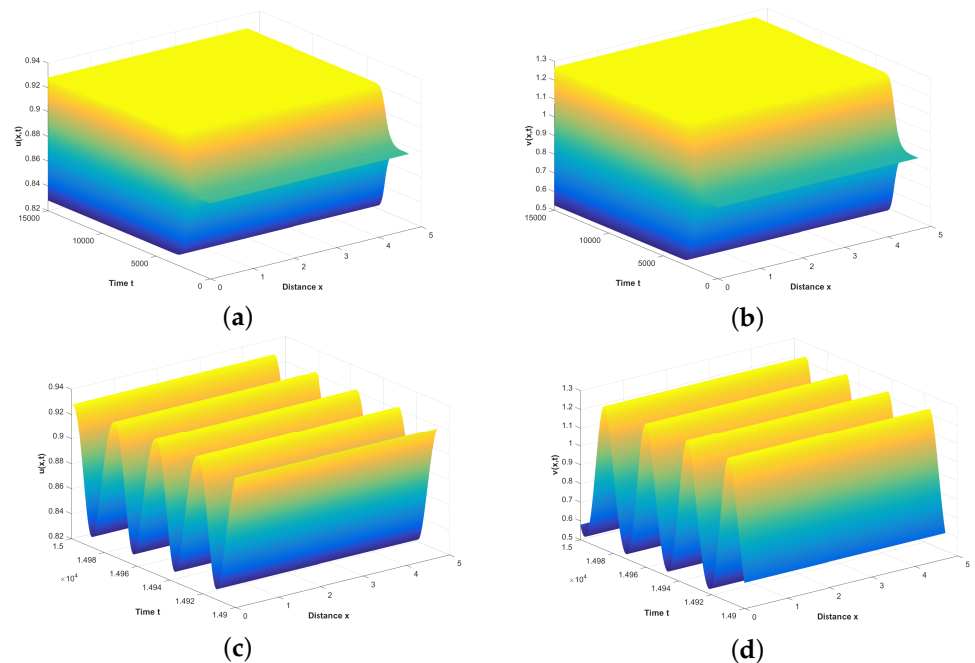


Figure 8. Numerical simulations for model (4) when  $\tau = 6.05 > \tau_0^1$  and for the initial values of  $u_0(x) = u_* + 0.001\cos x, v_0(x) = v_* - 0.001\cos x$ . (a,c) Prey. (b,d) Predator.

## 5. Conclusions and Discussion

In this work, we propose a delayed self-diffusive predator–prey model with a strong Allee effect on the prey and a fear effect on the predator. Unlike [17], in this paper, we added a time delay, self-diffusion, and nonlocal competition to the model, which makes the model more consistent with actual situations in nature and leads to homogeneous and inhomogeneous periodic solutions. By analyzing the eigenvalue spectrum, we studied the local stability of the coexisting equilibrium and the existence of Hopf bifurcation. By using the method of the center manifold theorem and the normal form method, we investigated the properties of Hopf bifurcation.

Next, we will discuss the influences of the fear effect and the strong Allee effect. The following conclusions can be drawn. Increasing the fear effect on the predator is beneficial to the uniform distribution of the prey and predator populations in space because the stable region of coexistence increases with the increase in the fear effect, and with the increase in the fear effect, a spatially inhomogeneous periodic solution appears first. However, when the fear effect is greater than a critical value, a spatially homogeneous periodic solution appears. However, increasing the strong Allee effect on the prey is not beneficial to the stability of the coexisting equilibrium because the stable region of coexistence decreases with the increase in the strong Allee effect. Whether the bifurcated periodic solution is spatially homogeneous or inhomogeneous depends on the strong Allee effect and the fear effect because with the increase in the strong Allee effect (or fear effect), a spatially inhomogeneous periodic solution appears first. However, when the strong Allee effect (or fear effect) is greater than a critical value, a spatially homogeneous periodic solution appears.

The main findings show that a strong Allee effect and the fear effect can be used to control the growth of prey and predator populations. For example, we could produce predation risk and affect the reproduction of sparrows by broadcasting their natural enemies' sounds (such as those of magpies, shrikes, sparrow eagles, etc.) during sparrows' entire breeding season. In this way, we can protect sparrows from direct killing and ensure that any effects on reproduction will only be ascribed to fear; this is the direction of our future research. Moreover, we found a Hopf–Hopf bifurcation point in the course of our research, which complicates the dynamic behavior of predator–prey systems and also requires further investigation.

However, questions remain as to whether emulating fear during an entire breeding season of a species is realistic, whether doing so would have other damaging consequences on the behavior of the species, and whether it would result in the species becoming accustomed with such sounds and no longer feeling fear (if the sounds perpetuate without any predation, the prey might consider that there is no danger after a while). This is also worth further research, especially in cooperation with biological experts.

**Author Contributions:** Y.X., J.Z. and R.Y. contributed to the study's conception and design. Material preparation, data collection, and analysis were performed by Y.X. and R.Y. All authors have read and agreed to the published version of the manuscript.

**Funding:** This research was supported by the Fundamental Research Funds for the Central Universities (grant No. 2572022DJ05), the Harbin Science and Technology Bureau Manufacturing Innovation Talent Project (CXRC20221110393), the Heilongjiang Science and Technology Department Provincial Key R&D Program Applied Research Project (SC2022ZX06C0025), the Heilongjiang Science and Technology Department Provincial Key R&D Program Guidance Project (GZ20220088), and the Postdoctoral Program of Heilongjiang Province (No.LBHQ21060).

**Data Availability Statement:** Data sharing is not applicable to this article, as no datasets were generated or analyzed during the current study.

**Conflicts of Interest:** The authors have no relevant financial or non-financial interest to disclose.

## References

1. Faria, T. Stability and Bifurcation for a Delayed Predator-Prey Model and the Effect of Diffusion. *J. Math. Anal. Appl.* **2001**, *254*, 433–463. [[CrossRef](#)]
2. Faria, T.; Magalhaes, L.T. Normal Forms for Retarded Functional Differential Equations with Parameters and Applications to Hopf Bifurcation. *J. Differ. Equ.* **1995**, *122*, 181–200. [[CrossRef](#)]
3. Faria, T. Normal forms and Hopf bifurcation for partial differential equations with delays. *Trans. Am. Math. Soc.* **2000**, *352*, 2217–2238. [[CrossRef](#)]
4. Yi, F.; Wei, J.; Shi, J. Bifurcation and spatiotemporal patterns in a homogeneous diffusive predator-prey system. *J. Differ. Equations* **2009**, *246*, 1944–1977. [[CrossRef](#)]
5. Song, Y.; Shi, Q. Stability and bifurcation analysis in a diffusive predator-prey model with delay and spatial average. *Math. Methods Appl. Sci.* **2022**, *46*, 5561–5584. [[CrossRef](#)]
6. Xiang, C.; Huang, J.; Wang, H. Bifurcations in Holling-Tanner model with generalist predator and prey refuge. *J. Differ. Equ.* **2023**, *343*, 495–529. [[CrossRef](#)]
7. Yang, R.; Nie, C.; Jin, D. Spatiotemporal dynamics induced by nonlocal competition in a diffusive predator-prey system with habitat complexity. *Nonlinear Dyn.* **2022**, *110*, 879–900. [[CrossRef](#)]
8. Yang, R.; Wang, F.; Jin, D. Spatially inhomogeneous bifurcating periodic solutions induced by nonlocal competition in a predator-prey system with additional food. *Math. Methods Appl. Sci.* **2022**, *45*, 9967–9978. [[CrossRef](#)]
9. Allee, W.C. Animal Aggregations. In *A Study in General Sociology*; University of Chicago Press: Chicago, IL, USA, 1931.
10. Stephens, P.A.; Sutherl, W.J. Consequences of the Allee effect for behaviour, ecology and conservation. *Trends Ecol. Evol.* **1999**, *14*, 401–405. [[CrossRef](#)] [[PubMed](#)]
11. Courchamp, F.; Clutton-Brock, T.; Grenfell, B. Inverse density dependence and the Allee effect. *Trends Ecol. Evol.* **1999**, *14*, 405–410. [[CrossRef](#)]
12. Berec, L.; Angulo, E.; Courchamp, F. Multiple Allee effects and population management. *Trends Ecol. Evol.* **2007**, *22*, 185–191. [[CrossRef](#)] [[PubMed](#)]
13. Bazykin, A. *Nonlinear Dynamics of Interacting Populations*; World Scientific: Singapore, 1998.
14. Panday, P.; Samanta, S.; Pal, N.; Chattopadhyay, J. Delay induced multiple stability switch and chaos in a predator-prey model with fear effect. *Math. Comput. Simul.* **2019**, *172*, 134–158. [[CrossRef](#)]
15. Qi, H.; Meng, X.; Hayat, T.; Hobiny, A. Bifurcation dynamics of a reaction-diffusion predator-prey model with fear effect in a predator-poisoned environment. *Math. Methods Appl. Sci.* **2022**, *45*, 6217–6254. [[CrossRef](#)]
16. Liu, T.; Chen, L.; Chen, F.; Li, Z. Dynamics of a Leslie-Gower Model with Weak Allee Effect on Prey and Fear Effect on Predator. *Int. J. Bifurc. Chaos* **2023**, *33*, 2350008. [[CrossRef](#)]
17. Liu, T.; Chen, L.; Chen, F.; Li, Z. Stability analysis of a Leslie-Gower model with strong Allee effect on prey and fear effect on predator. *Int. J. Bifurc. Chaos* **2022**, *32*, 2250082. [[CrossRef](#)]
18. Song, Y.; Peng, Y.; Zhang, T. The spatially inhomogeneous Hopf bifurcation induced by memory delay in a memory-based diffusion system. *J. Differ. Equ.* **2021**, *300*, 597–624. [[CrossRef](#)]
19. Akhmet, M.U.; Beklioglu, M.; Ergenc, T.; Tkachenko, V.I. An impulsive ratio-dependent predator-prey system with diffusion. *Nonlinear Anal. Real World Appl.* **2006**, *7*, 1255–1267. [[CrossRef](#)]
20. Liu, Y.; Wei, J. Double Hopf bifurcation of a diffusive predator-prey system with strong Allee effect and two delays. *Nonlinear Anal. Model. Control.* **2021**, *26*, 72–92. [[CrossRef](#)]
21. Yang, R.; Jin, D.; Wang, W. A diffusive predator-prey model with generalist predator and time delay. *AIMS Math.* **2022**, *7*, 4574–4591. [[CrossRef](#)]
22. Banerjee, M.; Takeuchi, Y. Maturation delay for the predators can enhance stable coexistence for a class of prey-predator models. *J. Theor. Biol.* **2017**, *412*, 154–171. [[CrossRef](#)]
23. Meng, X.; Jiao, J.; Chen, L. The dynamics of an age structured predator-prey model with disturbing pulse and time delays. *Nonlinear Anal. Real World Appl.* **2008**, *9*, 547–561. [[CrossRef](#)]
24. Britton, N.F. Aggregation and the competitive exclusion principle. *J. Theor. Biol.* **1989**, *136*, 57–66. [[CrossRef](#)]
25. Furter, J.; Grinfeld, M. Local vs. non-local interactions in population dynamics. *J. Math. Biol.* **1989**, *27*, 65–80. [[CrossRef](#)]
26. Geng, D.; Jiang, W.; Lou, Y.; Wang, H. Spatiotemporal patterns in a diffusive predator-prey system with nonlocal intraspecific prey competition. *Stud. Appl. Math.* **2021**, *48*, 396–432. [[CrossRef](#)]
27. Liu, Y.; Duan, D.; Niu, B. Spatiotemporal dynamics in a diffusive predator-prey model with group defense and nonlocal competition. *Appl. Math. Lett.* **2020**, *103*, 106175. [[CrossRef](#)]
28. Geng, D.; Wang, H. Normal form formulations of double-Hopf bifurcation for partial functional differential equations with nonlocal effect. *J. Differ. Equ.* **2022**, *2022*, 741–785. [[CrossRef](#)]
29. Djilali, S. Pattern formation of a diffusive predator-prey model with herd behavior and nonlocal prey competition. *Math. Methods Appl. Sci.* **2020**, *43*, 2233–2250. [[CrossRef](#)]
30. Pati, N.C.; Ghosh, B. Stability scenarios and period-doubling onset of chaos in a population model with delayed harvesting. *Math. Methods Appl. Sci.* **2022**. [[CrossRef](#)]
31. Barman, B.; Ghosh, B. Explicit impacts of harvesting in delayed predator-prey models. *Chaos Solitons Fractals* **2019**, *122*, 213–228 [[CrossRef](#)]

32. Ghosh, B.; Barman, B.; Saha, M. Multiple dynamics in a delayed predator-prey model with asymmetric functional and numerical responses. *Math. Methods Appl. Sci.* **2023**, *46*, 5187–5207. [[CrossRef](#)]
33. Wu, J. *Theory and Applications of Partial Functional Differential Equations*; Springer: Berlin/Heidelberg, Germany, 1996.
34. Hassard, B.D.; Kazarinoff, N.D.; Wan, Y.H. *Theory and Applications of Hopf Bifurcation*; Cambridge University Press: New York, NY, USA, 1981.

**Disclaimer/Publisher's Note:** The statements, opinions and data contained in all publications are solely those of the individual author(s) and contributor(s) and not of MDPI and/or the editor(s). MDPI and/or the editor(s) disclaim responsibility for any injury to people or property resulting from any ideas, methods, instructions or products referred to in the content.